

Luminescent Oxide Materials Obtained by the Extraction Pyrolytic Method

T. N. Patrusheva, A. S. Aleksandrovskii, A. A. Khval'ko, Yu. V. Kolovskii,
A. V. Polyushkevich, and A. I. Khol'kin

Siberian Federal University, Svobodnyi pr. 79, Krasnoyarsk, 660041 Russia

Institute of Physics, Siberian Branch, Russian Academy of Sciences, Krasnoyarsk, Akademgorodok, 660036 Russia

Kurnakov Institute of General and Inorganic Chemistry, Russian Academy of Sciences,

Leninskii pr. 31, Moscow, 119991 Russia

e-mail: pat55@mail.ru

Received June 27, 2009

Abstract—Luminescent $Y_{1.74}Eu_{0.16}Bi_{0.1}O_3$ films have been obtained by extraction pyrolytic method. The formation of a crystalline structure in the film upon isothermal annealing in air at 600–650°C was established by X-ray diffraction. Single-phase $Y_{1.74}Eu_{0.16}Bi_{0.1}O_3$ films begin to exhibit luminescent properties after pyrolysis at 500°C; the intensity of luminescence increases with increasing temperature. The films annealed at 800°C consists of defect-free homogeneous crystallites with sizes of about 0.7 μm and demonstrates high luminescence intensity.

Keywords: extraction pyrolytic method, luminescent films, X-ray diffraction, luminescence spectra

DOI: 10.1134/S0040579512040069

INTRODUCTION

Luminescent materials have found wide application in information imaging, lighting, and indication [1]. Using coatings based on these materials allows one to increase the luminescence and contrast of the images of various objects, which in turn improves the quality and efficiency of monitoring and (or) diagnosing the state of the latter [2]. In medicine, special compositions of phosphors are developed to simplify disease diagnosing. The visualization of the image in green light has a clear advantage in roentgenography [3]. In criminalistics, nanosized luminescent powders allow one to reveal highly accurate fingerprints [4]. Some systems of X-ray sensors are based on luminescent materials. The wide range of applications of luminescent materials has shaped the requirements for the optical properties and compatibility with the objects for which they are created. For example, when used in spacecraft, luminescent materials and coatings on their basis should retain their optical properties under vacuum conditions, at large temperature drops, under cosmic radiation, etc. for decades [5].

Two large classes of phosphors are known, namely, sulfide and oxide phosphors. The sulfide materials are sensitive to electrophilic factors, such as H^+ and CO_2 ; consequently, the sulfide phosphors are unstable in CO_2 , O_2 , and wet environments, undergoing hydrolytic decomposition [6]. This fact was repeatedly confirmed in practice, which forms the basis for definite

limitations in using sulfide phosphors. A glowing example of oxide phosphors is zinc oxide, which has piezoelectric properties, high electron conductivity, and optical transparency. Zinc oxide is a promising material for creating semiconductor sources of visible and UV light [7].

At present, there is a large set of mixed oxide luminescent materials activated by europium, manganese, and zinc, for example, $YVO_4:Eu$, $Zn_2SiO_4:Mn$, $ZnO:zn$, $Y_2O_3:Eu$, etc. [1–9]. Mixed oxides are promising materials in view of their stability, especially in a vacuum and at abnormal temperatures. Reliability, long service life, low power requirements, and small sizes are typical of the given materials and, correspondingly, of devices that use these phosphors. Compounds that simultaneously contain a rare-earth element and bismuth are of special interest. Information on europium and bismuth compounds is scarce and, in some cases, discrepant. Compounds of rare-earth elements are characterized by broad emission ranges and short relaxation times.

The $Y_2O_3:Eu$ material is a widely used phosphor under excitation with 254-nm light. The maximum luminescence occurs in the 610-nm region, and all other lines are weak [8]. Excitation with ultraviolet emitting diodes in the range of 360–400 nm is due to the absorption in high-lying 4f–4f transitions.

At room temperature, Eu–BM–O compounds show intense red luminescence. The luminescence spectra of mixed compounds are due to transitions

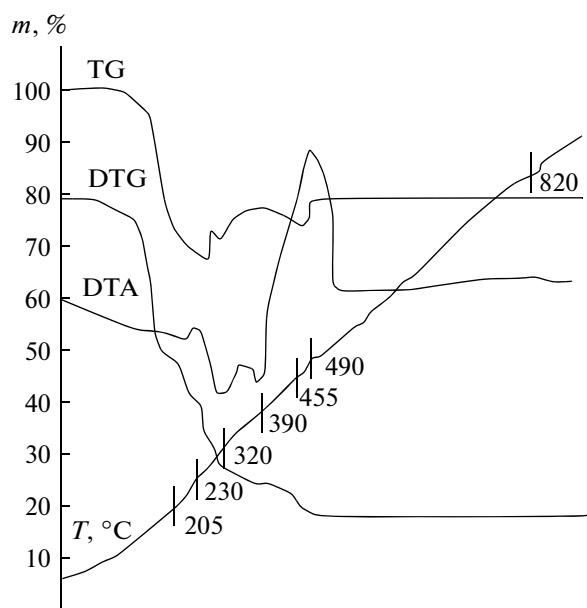


Fig. 1. Thermal decomposition of Bi carboxylate in air.

inside the 4f shell of Eu^{3+} and have discrete structures. It was shown [8] that the introduction of Bi^{3+} does not change fluorescence intensity of Eu^{3+} at a Bi^{3+} content of up to 10%.

Solid phase interactions in stoichiometric oxide mixtures of europium and bismuth of high purity yield an oxide $(\text{Y}_{1.84}\text{Eu}_{0.16})\text{O}_3$ after 24 h in air at 1300–1650°C [10]. The increase in particle size from 300 nm to 4 μm was observed with increasing caking temperature.

The synthesis method has a significant effect on the sizes of grains, surface area, and defect structure of the materials. The luminescence intensity of the phosphors synthesized by the coprecipitation method was higher than that of the phosphors synthesized by the reaction of the solid oxides at different temperatures [11].

Various methods are used to produce thin phosphor films, including the sol-gel method, hydrothermal synthesis, and laser evaporation. It should be noted that, during phosphor preparation, the use of any of the above methods to achieve high luminescence brightness requires high-temperature treatment, which was aimed, first, at the formation of optically active centers in the course of the diffusion of corresponding impurities, which creates the necessary intrinsic defects and, second, at decreasing the density of linear and surface defects and the formation of crystals of the required size [12].

EXPERIMENTAL

To obtain the luminescent $\text{Y}_{1.74}\text{Eu}_{0.16}\text{Bi}_{0.1}\text{O}_3$ films, the extraction pyrolytic method was applied [13]. Prepared solutions of Y, Eu, and Bi extracts were mixed in stoichiometric proportions of 1.74 : 0.16 : 0.1. Organic

salts of metals were deposited on the substrate and subjected to pyrolysis, forming the corresponding oxides and gaseous decomposition products, predominantly CO_2 . The main parameter of the process is the temperature of decomposition of the compounds. The thermal decomposition of the Bi, Eu, and Y extracts were studied using a Q-1000 Paulik–Paulik–Erdey thermal analyzer.

The X-ray diffraction analysis of intermediates and final products was conducted on a DRON-4-07 diffractometer (Russia) with a GUR-9 goniometer (Russia) using copper-filtered $\text{CuK}\alpha$ radiation with the rotation of the sample normal to its plane.

Images of films were obtained by atomic-force microscopy in air using a Solver P47 multimode probe-scanning microscope (NT-MDT) in semi-contact mode with a silicon cantilever with a constant rigidity of about 5 N/m.

The study of the luminescence of the samples was performed using excitation at wavelengths of 355 nm (a ultraviolet DTL-LCS-374QT laser on Nd:YAG) and 476 nm (argon laser), as well as using an AMINCO-Bowman AB2 luminescent spectrometer.

RESULTS AND DISCUSSION

The dependence of the heat of decomposition on the composition of extracts was studied. Curves of the thermal decomposition of Bi carboxylate extracted by a mixture of the highest isomers of carboxylic acids (HIA) in air are shown in Fig. 1. The thermal decomposition of the extract occurs in three stages. The release of chemically bound water takes place at 130°C, and the release of excess of carboxylic acids occurs at 230–320°C; the decomposition of bismuth carboxylates begins at 390°C and is completed at 450°C.

The thermoanalytical profiles of europium and yttrium extracts have a similar character and analogous pyrolysis stages. All of the components pass into solid oxide phases at 430–450°C.

The $\text{Y}_{1.74}\text{Eu}_{0.16}\text{Bi}_{0.1}\text{O}_3$ film was deposited on a glass substrate by the wetting method followed by drying and pyrolysis. Pyrolysis was carried out at 450°C. The wetting–pyrolysis cycle was repeated 15 times to attain a film thickness of around 500 nm.

Each subsequent layer filled pores in the previous layer and a uniform film was formed after three repetitions. The films were annealed at temperatures of 500, 550, 600, and 650°C for 1–2 h.

After pyrolysis, the films were gray and, after 10 min of annealing, they became white, which indicates the removal of carbon. Crystallization begins at 450°C and the X-ray diffraction pattern of the samples demonstrate low, broad peaks, which suggests small particle sizes. With an increasing annealing temperature, the peaks of the X-ray diffraction pattern become narrower and their intensity increases.

Figure 2 shows the X-ray diffraction pattern of the $Y_{1.74}Eu_{0.16}Bi_{0.1}O_3$ film annealed at 650°C for 2 h.

The X-ray diffraction analysis of the films on glass showed the presence of $Y_{1.74}Eu_{0.16}Bi_{0.1}O_3$ phase peaks, which correspond to the data of the International Centre for Diffraction Data (ICDD).

Further investigations of the materials demonstrated that the $Y_{1.74}Eu_{0.16}Bi_{0.1}O_3$ films already start to show luminescent properties after annealing at 500°C. The intensity of the luminescence of this material increases with increasing temperature of annealing. The $Y_{1.74}Eu_{0.16}Bi_{0.1}O_3$ film on polycor was annealed at temperatures of 700, 800, 900, and 1000°C. All of the samples showed intense luminescence under UV irradiation.

The results of atomic force microscopy show that the $Y_{1.74}Eu_{0.16}Bi_{0.1}O_3$ film obtained after annealing at 800°C for 1 h (Fig. 3) consists of homogeneous, cylindrical grains around 700 nm in size, which corresponds to the grain sizes of bulk phosphor. Materials with large grains are known to have similar high luminescence parameters. However, a reduction in the sizes of grains to 10–100 nm results in the emergence of quantum effects. The presence of large and small grains promotes an increase in the film density, as well as can lead to a twofold luminescence effect.

A visual evaluation of luminescent properties of the obtained samples was carried out using a UV laser. $Y_{1.74}Eu_{0.16}Bi_{0.1}O_3$ samples annealed at 650°C were found to shine significantly more weakly than samples annealed at 800–900°C.

The luminescence of the samples annealed at low temperatures has a significant blue component, which should be identified as the luminescence of trivalent bismuth, as well as a red-toned glow. The samples annealed at 900°C show much more intense luminescence of orange-red color. It should be noted that raising the temperature of annealing above the melting point of bismuth oxide (820°C) may lead to the evaporation of bismuth oxide or its interaction with the substrate; its amount in the film material can be changed accordingly.

The luminescent spectra of samples annealed at 800 (sample with red-blue glow) and 900°C (sample with red glow) during excitation with an argon laser at a wavelength of 476 nm are shown in Fig. 4. The spectra of sample 1 are shown by a solid line and the spectra of sample 2 are shown by dotted line (Figs. 4–7).

Luminescence spectra at 450–650 nm have a form typical of trivalent europium luminescence in crystalline matrices with maximums around 610 nm (Fig. 4). In addition, atypical lines at 692.7 and 694.2 nm were observed for trivalent europium. In sample 2, dark red luminescence at wavelengths of 692.7 and 694.2 nm dominated over luminescence in the orange-red area. Characteristic europium lines were also observed in the spectrum of sample 2, but they have significantly lower intensity.

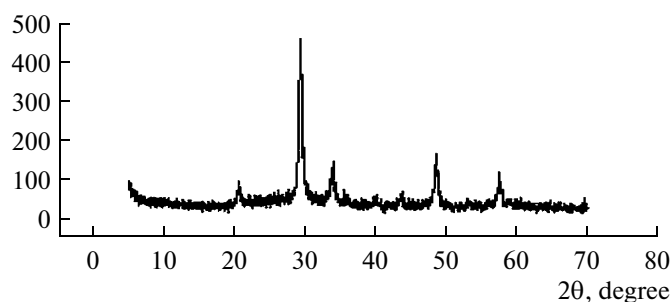


Fig. 2. X-ray diffraction pattern of the $_{1.74}Eu_{0.16}Bi_{0.1}O_3$ film annealed at 650°C for 2 h.

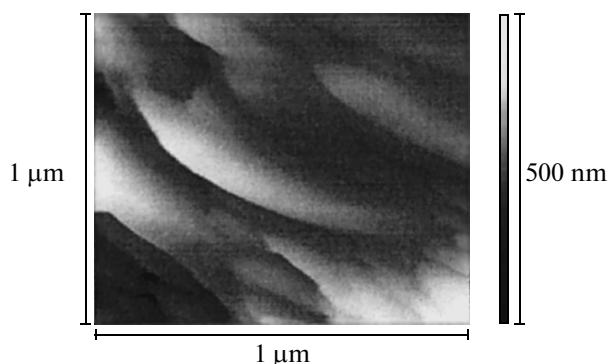


Fig. 3. $_{1.74}Eu_{0.16}Bi_{0.1}O_3$ film annealed at 800°C for 1 h.

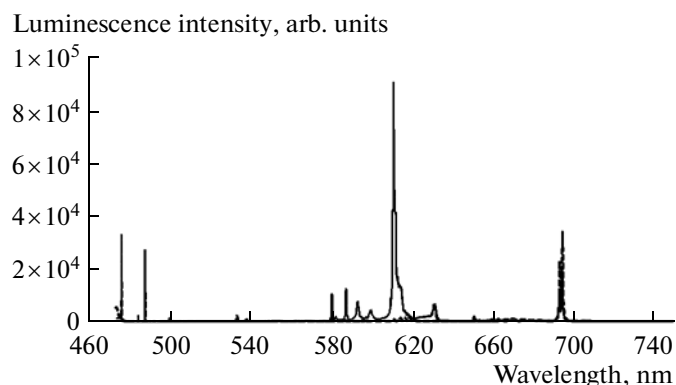


Fig. 4. Luminescence spectra of $_{1.74}Eu_{0.16}Bi_{0.1}O_3$ samples 1 (continuous line) and 2 (dotted line) upon excitation at 476 nm.

The luminescence spectra obtained using an AMINCO-Bowman AB2 spectrometer under 240-nm excitation fall in the area of the charge transfer of trivalent europium (Figs. 6–8).

In general, upon excitation at this wavelength, as well as upon excitation at 476 nm, trivalent europium luminescence has the same form. A difference is only exhibited near 700 nm, where additional peaks come into view that may be related to the formation of complex oxide phases. Figure 8 presents spectra of lumi-

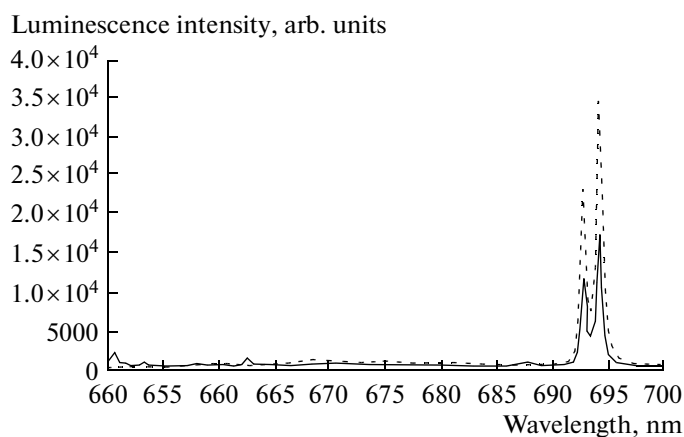


Fig. 5. Longwave part of the luminescence spectra of $Y_{1.74}Eu_{0.16}Bi_{0.1}O_3$ samples 1 (continuous line) and 2 (dotted line) at 476-nm excitation.

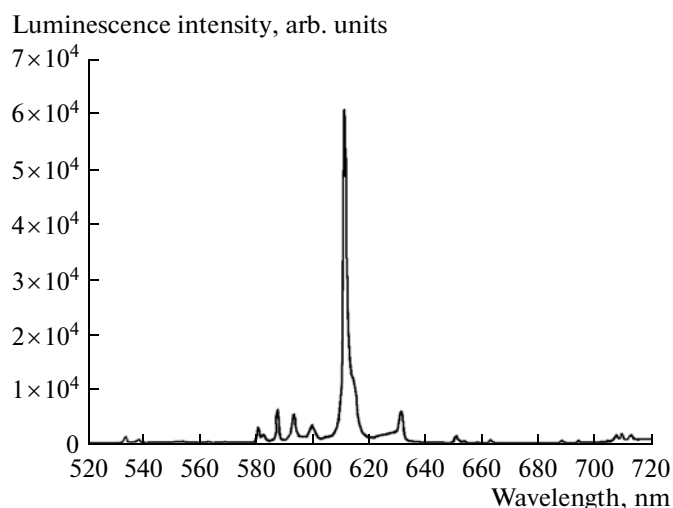


Fig. 6. Luminescence spectra of $Y_{1.74}Eu_{0.16}Bi_{0.1}O_3$ samples 1 (continuous line) and 2 (dotted line) obtained using a spectrometer AMINCO-Bowman AB2 at 240 nm excitation.

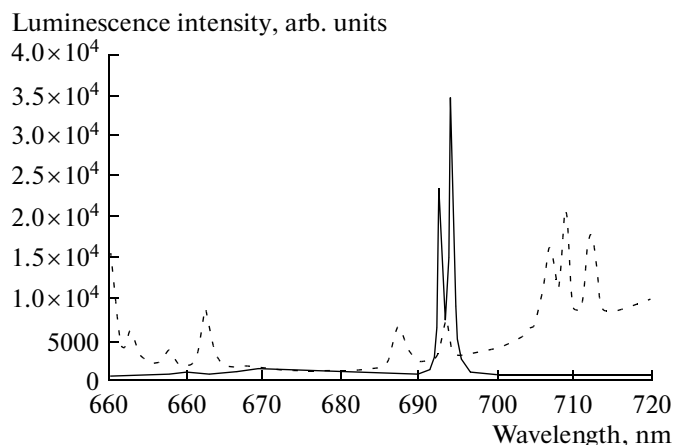


Fig. 7. Longwave part of luminescence spectra of $Y_{1.74}Eu_{0.16}Bi_{0.1}O_3$ obtained on a spectrometer AMINCO-Bowman AB2 at 240 nm (dotted line) and 476 nm (continuous line) excitation.

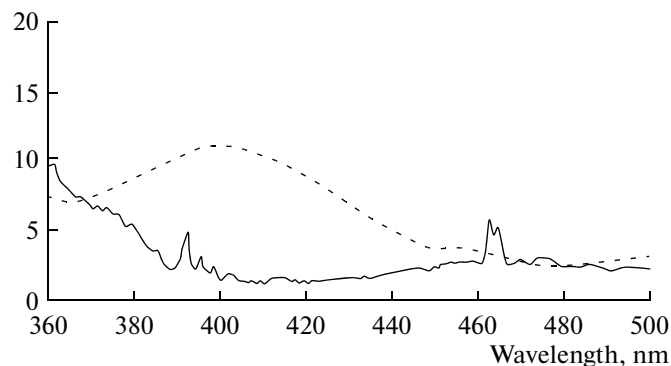


Fig. 8. Excitation spectra of luminescence at 612 (continuous line) and 693 nm (dotted line) excitation.

nescence excitation at wavelengths of 612 (transition ${}^5D_0-{}^7F_2$ of the Eu^{3+} ion) and 693 nm. The spectrum of luminescence excitation at a wavelength of 612 nm corresponds to an expected spectrum of trivalent europium; in particular, it contains peaks at wavelengths of 392 (${}^7F_0-{}^5L_6$) and 464 (${}^7F_0-{}^5D_2$) nm. The spectrum of luminescence excitation at a wavelength of 693 nm is radically different from the expected spectrum of trivalent europium; in particular, it does not contain the above peaks. This indicates that luminescence in the 693-nm area is not related to the europium ion.

Thus, the red $Y_{1.74}Eu_{0.16}Bi_{0.1}O_3$ film luminescence annealed at 900°C is typical of trivalent europium, and red-blue luminescence of the $Y_{1.74}Eu_{0.16}Bi_{0.1}O_3$ film annealed at 800°C is due to the influence of bismuth

ions. The film annealed under temperature-gradient conditions at 800–900°C may have areas with different glows.

CONCLUSIONS

The luminescent $Y_{1.74}Eu_{0.16}Bi_{0.1}O_3$ films were obtained using the extraction pyrolytic method. X-ray analysis shows crystallization of the $Y_{1.74}Eu_{0.16}Bi_{0.1}O_3$ phase at just 650°C. The degree of crystallinity grows at increasing temperature. The investigation of the microstructure of samples annealed at 800°C demonstrated the presence of 0.7- μ m grains, which is typical of materials with high luminescence intensity.

The samples of luminescence typical of trivalent bismuth and trivalent europium in the samples synthe-

sized in various conditions. The optimum conditions for synthesis of the luminescent $_{1.74}\text{Eu}_{0.16}\text{Bi}_{0.1}\text{O}_3$ film were found in this investigations, namely, annealing at 800°C for 2 h. The demonstrated method allows one to soften the technological parameters of preparation of luminescent materials and to broaden their range of optical characteristics.

ACKNOWLEDGMENTS

The work was supported by the Russian Foundation for Basic Research project, no. 10–03–00188a).

REFERENCES

1. Bartko, A.P., Peyser, L.A., and Dickson, R.M., Observation of Dipolar Emission Patterns from Isolated $\text{Eu}^{3+}:\text{Y}_2\text{O}_3$ Doped Nanocrystals: New Evidence for Single Ion Luminescence, *Chem. Phys. Lett.*, 2002, nos. 5–6, p. 459.
2. Kolovski, Y.V. and Ten, V.P., New Developments of Methods of Highly Precision Measurements of 3rd Order Deviation Parameters of Surface Shape, *Proc. ITT Conf. ITT-98*, Ohio, USA, 1998, p. 383.
3. Gopelik, F.G.K., Use of “Blue” and “Green” Systems of Image Visualization in X-ray Spectroscopy, *Med. Tekh.*, 2003, no. 5, p. 39.
4. Bapladyan, B.Kh., Voloboi, A.G., and V'yukova, N.I., Modeling of Illumination and Synthesis of Photorealistic Images with the Use of Internet Technology, *Prog-pammirovanie*, 2005, no. 5, p. 66.
5. Kolovskii, Yu.V., Intelligent Systems of Functional Diagnostics and Control of Onboard Hybrid Mirror Antennas, *Mezhd. konf. po myagkim vychisleniyam i izmepeniyam* (Proc. Int. Conf. on Soft Calculations and Measurements), St. Petersburg, 2003, vol. 2, p. 63.
6. Kazarbina, T.V., Voponina, L.I., and Kostikova, V.A., *Materialy dlya istochnikov sveta i svetotekhnicheskikh izdelii* (Materials for Light Sources and Lighting Articles), Saransk, 1993, p. 111.
7. Lee, Yun-Ju, Ruby, D.S., Peters, D.W., et al., ZnO Nanostructures as Efficient Antireflection Layers in Solar Cells, *Nano Lett.*, 2008, vol. 8, no. 5, p. 1505.
8. Kalinovskaya, I.V. and Kapasev, V.E., Synthesis and Spectroscopic Properties of Mixed Compounds of Europium and Bismuth with Cinnamic Acid, *Russ. J. Inorg. Chem.*, 1999, vol. 44, no. 8, p. 1173.
9. Sokolov, V.V. and Uskov, E.M., Bright Red High-Transmittance Phosphor Based on $\text{NaY}_{1-x}\text{Eu}_x(\text{MoO}_4)_2$, *Khim. Interes. Ust. Pazv.*, 2000, vol. 8, nos. 1–2, p. 281.
10. Gaiduk, M.I., Zolin, V.F., and Gaigepova, L.S., *Spektry lyuminesentsii evropiya* (Europium Luminescence Spectra), Moscow: Nauka, 1974.
11. Srivastava, A.M. and Ronda, C.R., Phosphors, *Electrochem. Soc. Interface*, 2003, no. 3, p. 49.
12. Petushkov, A.A., Shilov, S.M., and Pak, B.N., Dimensional Features of the Luminescence of Europium(III) Chloride Nanoparticles in a Porous Glass Matrix, *Tech. Phys. Lett.*, 2004, vol. 30, no. 11, p. 894.
13. Khol'kin, A.I. and Patpusheva, T.N., *Ekstraktsionno-piroliticheskii metod: Poluchenie oksidnykh funktsional'nykh materialov* (Extraction–Pyrolytic Method: Production of Functional Oxide Materials), Moscow: Kom. Kniga, 2006.